

## THE TOPOTACTIC TRANSFORMATION OF TUNGSTEN OXIDE TO A CUBIC TUNGSTEN CARBIDE

Jae Sung LEE

Department of Chemical Engineering, Pohang Institute of Science and Technology, P.O.Box 125, Pohang, Korea

(Received 22 August 1988 • accepted 18 January 1989)

**Abstract**—The solid transformation of tungsten trioxide to a cubic tungsten carbide via nitride has been studied. Product carbide particles possessed specific surface area of *ca.* 90 m<sup>2</sup>g<sup>-1</sup> and average diameter of *ca.* 4 nm. Transmission electron microscope (TEM) exhibited that these particles formed porous aggregates with a spotty electron diffraction pattern. This provides an evidence that the topotactic solid transformation has been involved.

### INTRODUCTION

Tungsten carbide exhibits platinum-like catalytic behavior for some surface and catalytic reactions [1,2]. Due to this interesting property of tungsten carbide, considerable efforts have been directed towards the development of procedures to prepare tungsten carbide with high specific surface area and high purity [3]. A new method developed by Boudart and co-workers involves temperature-programmed reactions (TPR) of a metal oxide with ammonia forming a metal nitride followed by temperature-programmed carburization of the nitride with CH<sub>4</sub>-H<sub>2</sub> mixture to form uncommon metastable cubic carbide [4,5]. When the starting material was MoO<sub>3</sub> with specific surface area (S<sub>g</sub>) less than 1 m<sup>2</sup>g<sup>-1</sup>, cubic Mo<sub>2</sub>N and αMoC<sub>1-x</sub> powders with S<sub>g</sub> of *ca.* 200 m<sup>2</sup>g<sup>-1</sup> were synthesized [5]. The transformations of oxide-to-nitride and nitride-to-carbide were shown to be topotactic as {100} planes of Mo<sub>2</sub>N were parallel to {010} planes of MoO<sub>3</sub>, and the face-centered cubic (fcc) structure of Mo<sub>2</sub>N remained unaltered when αMoC<sub>1-x</sub> was formed.

Although a high S<sub>g</sub> tungsten carbide could be produced by the same procedure [4], it was not determined if the topotactic transformation was involved in the synthesis as well. It is of interest because the preparation temperature of tungsten carbide is at least 100 K higher than that of molybdenum counterpart. For this purpose, the present study employs transmission electron microscopy(TEM) coupled with selected area electron diffraction (SAD), which has been proved to be an ideal tool to identify topotaxy in the case of the molybdenum oxide-to-nitride transformation [6]. The results of catalytic reactions on this tungsten carbide

βW<sub>2</sub>C will be published elsewhere [7].

### EXPERIMENTAL

#### 1. Sample preparation

The procedure to prepare βW<sub>2</sub>C powders is summarized schematically in Fig. 1. About 100 mg of high purity WO<sub>3</sub> (99.998%, Johnson-Matthey) was loaded onto a fritted disc fixed in a quartz cell. A stream of NH<sub>3</sub> (Matheson, anhydrous) at atmospheric pressure was flown through the cell at a rate of 100 μmol s<sup>-1</sup>. Then the temperature of the sample was varied by a controller/programmer coupled to an electric furnace containing the cell. Following rapid heating to 870 K, the sample was further heated up to 1050 K by TPR with a linear heating rate of 30 K h<sup>-1</sup>. This first step of preparation yields fcc W<sub>2</sub>N powder with S<sub>g</sub> of 91 m<sup>2</sup>g<sup>-1</sup>. In the second step, W<sub>2</sub>N powder cooled to 870 K were carburized by the same TPR used for nitride preparation with a gas mixture of 80% CH<sub>4</sub> (deoxygenated by passage through an MnO trap) and H<sub>2</sub> (Liquid Carbonic) purified by Pd-diffusion, flowing at 80 μmol s<sup>-1</sup>. The surface of tungsten carbide thus obtained is completely covered by polymeric carbon, and does not chemisorb CO or H<sub>2</sub>. In the final step of preparation, this polymeric carbon is selectively removed by H<sub>2</sub> treatment at 1000 K. The CH<sub>4</sub> produced from the hydrogenolysis of polymeric carbon was continuously monitored by a gas chromatograph. When the maximum CH<sub>4</sub> concentration was observed, the sample was immediately quenched to room temperature (RT) by removing the furnace.

#### 2. Gas adsorption and X-ray diffraction

To measure the gas adsorption, the preparation cell

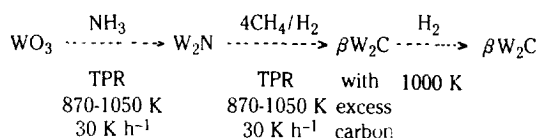


**Fig. 1. Preparation of  $\beta\text{W}_2\text{C}$  from  $\text{WO}_3$  by temperature-programmed reaction (TPR).**

was isolated and transferred to a volumetric adsorption system equipped with a Texas Instruments differential pressure gauge. To measure the amount of CO adsorption, the cell was evacuated to  $10^{-4}$  Pa at 670 K, and various amounts of CO were dosed sequentially at RT to obtain a first adsorption isotherm. The cell was then evacuated again to  $10^{-4}$  Pa at RT for 0.5 h to remove the weakly adsorbed CO. Then a second adsorption isotherm was taken to measure the amount of weakly adsorbed CO. The linear portion of the isotherms was extrapolated to zero pressure and the difference between the two extrapolated values was taken as the amount of strongly chemisorbed CO. To determine  $\text{H}_2$  chemisorption a similar procedure was employed, but only the first isotherm was taken. A physical isotherm of  $\text{N}_2$  was obtained and analyzed by means of the BET method to determine  $S_g$ . The bulk structure of the tungsten carbide was checked by powder x-ray diffraction. The widths of (111) and (200) diffraction peaks at half-maximum were used to estimate the average crystal size. Both peaks yielded similar values of  $D_c$ . Since the sample is pyrophobic when suddenly exposed to air, it was passivated at RT with flowing 1%  $\text{O}_2$  in He before removal from the preparation cell for the x-ray diffraction measurement.

### 3. Transmission electron microscopy

For transmission electron microscopy (TEM), the passivated sample were dispersed ultrasonically in ethanol and then deposited on a TEM grid that had been coated with  $\text{S}_a$  holey carbon film. A Hitachi 500H microscope was operated at 100 kV.

## RESULTS AND DISCUSSION

Table 1 shows characterization data for  $\beta\text{W}_2\text{C}$ . After preparation, the specific surface area  $S_g$  determined by the  $\text{N}_2$  BET method was  $90 \text{ m}^2\text{g}^{-1}$ . This corresponds to particle size  $D_p$  of ca. 4 nm. The amount of chemisorbed CO and  $\text{H}_2$  was found by extrapolating isotherms to zero pressure. In the case of CO chemisorption, only the fraction that could not be evacuated at RT was regarded as being irreversibly chemisorbed at this temperature. The number density  $n_{\text{CO}}$  or  $n_{\text{H}_2}$  was calculated as the amount of CO or  $\text{H}_2$  chemisorbed per unit BET area.

**Table 1. Characterization data of  $\beta\text{W}_2\text{C}$  powder**

Specific surface area, $S_g/\text{m}^2\text{g}^{-1}$	90
Chemisorption at RT/ $\mu\text{mol g}^{-1}$	
CO	351
$\text{H}_2$	224
Number density/ $10^{14} \text{ cm}^{-2}$	
$n_{\text{CO}}$	2.35
$n_{\text{H}_2}$	1.50
Particle size/nm	
$D_p$ by BET <sup>a</sup>	4
$D_c$ by X-ray <sup>b</sup>	4

a:  $D_p = 6/\rho S_g$ ,  $\rho$  = density of the solid.

b:  $D_c = \lambda/(\beta \cos \theta)$ ,  $\lambda$  = wavelength of  $\text{CuK}\alpha$  X-ray radiation,  $\theta$  = Bragg angle,  $\beta$  = halfwidth of diffraction peak corrected for  $\text{K}\alpha$  radiation and instrumental broadening.

The X-ray diffraction peaks indicated a FCC crystal structure with a cubic lattice parameter of 418 pm. An average crystal size  $D_c$  of 4 nm was estimated from the application of Scherrer's equation to the width of the x-ray diffraction peak at half-maximum, corrected for instrumental broadening. Agreement with  $D_p$  from BET area is good.

In order for  $\beta\text{W}_2\text{C}$  to be an efficient catalyst, it should not only have a large surface area but should also have a surface free of any contamination. The most common surface contaminants in metal carbides are oxygen and polymeric carbon. Kojima et al. [8] found that evacuation above 1270 K activated TaC, TiC, and WC for the hydrogenation of ethylene due to the removal of oxygen or oxide. The polymeric carbon is more difficult to avoid because it originates from the preparation itself. It was shown that the presence of polymeric carbon on WC suppressed the chemisorption of  $\text{H}_2$  [2]. According to thermodynamics shown in Fig. 2 graphite formation by  $\text{CH}_4$  decomposition is favored for  $\text{CH}_4\text{-H}_2$  mixture with more than ca. 5%  $\text{CH}_4$  at 1050 K, the highest temperature of the preparation. Below 5% of  $\text{CH}_4$  concentration, tungsten carbide is still stable relative to the metal. However, it was found that  $\beta\text{W}_2\text{C}$  formed under this condition contained a metallic W phase probably due to the slow diffusion of carbon atoms into the bulk. A  $\beta\text{W}_2\text{C}$  sample with a metal impurity always possesses a lower  $S_g$  than that of a pure sample.

The 80%  $\text{CH}_4$  in  $\text{H}_2$  was chosen as the carburization mixture knowing that the surface of  $\beta\text{W}_2\text{C}$  would be completely covered by polymeric carbon. As expected, it did not chemisorb CO or  $\text{H}_2$  at RT right after carburization. The  $\text{H}_2$  treatment at 1000 K provides a

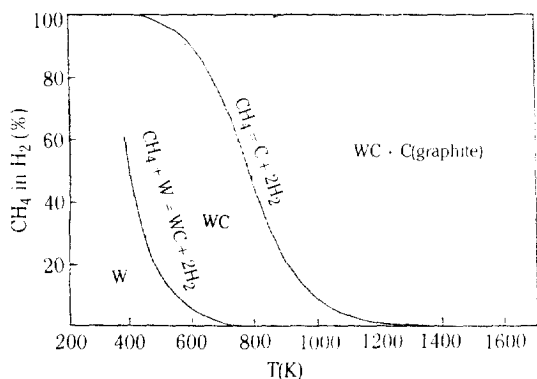


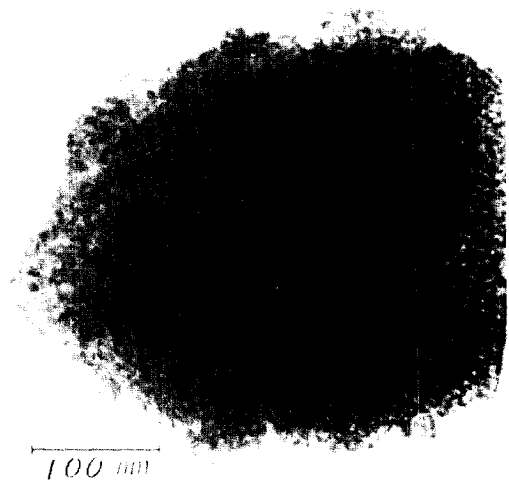
**Fig. 2. Thermodynamics of carburization with a  $\text{CH}_4$ - $\text{H}_2$  mixture at atmospheric pressure.**

Thermodynamic data were obtained from Barin, I. and Knacke, O.: "Thermochemical Properties of Inorganic Substances", Springer-Verlag, Heidelberg, 1973.

method to remove polymeric carbon from the surface of this sample. The treatment should be interrupted immediately after observing maximum  $\text{CH}_4$  concentration. Further treatment beyond this maximum results in decrease in  $S_g$  and CO chemisorption since it starts to destroy underlying carbide structure.

It is believed that an appreciable amount of polymeric carbon still remains on the surface of  $\beta\text{W}_2\text{C}$  even after treatment with  $\text{H}_2$ , because the removal of surface carbon was interrupted when the maximum  $\text{CH}_4$  formation was observed. However, a large fraction of the surface is clean as indicated by CO and  $\text{H}_2$  chemisorption. Assuming that the surface consists of equal portions of the low index planes, we can expect the density of metal atoms on a clean  $\beta\text{W}_2\text{C}$  surface to be  $1.1 \times 10^{15} \text{ cm}^{-2}$ . With adsorption stoichiometry of 1:1 for CO molecule and H atom, W atoms chemisorbing CO molecules or H atoms correspond to ca. 23% and 27%, respectively. Benziger et al. [9] showed that a considerable amount of CO could be removed below RT by flash desorption. Thus CO uptake reported here may represent a lower bound estimation of the number of clean W atoms. The remaining portion of surface W atoms which was not titrated by CO or  $\text{H}_2$  is believed to be covered by the polymeric carbon.

Below 2800 K, the stable tungsten carbide phases include simple hexagonal  $\alpha\text{WC}$  and hexagonal close-packed  $\text{W}_2\text{C}$  [10]. The FCC carbide of interest here ( $\beta\text{W}_2\text{C}$ ) is metastable and has been obtained at low temperature only by rapid quenching of W-C mixture from temperatures above 2800 K [11]. The preparation method employed here thus allow us to obtain this un-



(a)



(b)

**Fig. 3. A Small aggregate of  $\beta\text{W}_2\text{C}$  under a transmission electron microscope.**

(a) Bright-field image.

(b) Corresponding selected area diffraction pattern. The spots show the  $\{100\}$  orientation.

usual phase at much lower temperatures. As has been demonstrated elsewhere for the case of FCC molybdenum carbide [4,5], the solid transformations involved in our preparation appear to be *topotactic* because of the relationship of crystal structure between the parent and the product throughout the bulk of the solid [12,13]. Thus, the cubic lattice of  $\beta\text{W}_2\text{C}$  is simply inherited from cubic  $\text{W}_2\text{N}$  which, in turn, has developed its cubic lattice from the *oriented* (instead of *random*) nucleation of its phase relative to the parent  $\text{WO}_3$  crystal. The large surface area of  $\text{W}_2\text{N}$  ( $91\text{ m}^2\text{g}^{-1}$ ) is also a consequence of a topotaxy of  $\text{WO}_3$ -to- $\text{W}_2\text{N}$  transformation [5]. During the formation of  $\beta\text{W}_2\text{C}$ , it appears that nitrogen atoms are replaced with carbon atoms without disturbing the W lattice, thus preserving a high  $S_g$  or a small particle size of  $\text{W}_2\text{N}$ .

An ideal tool to identify topotaxy during a reaction of powdered solids is TEM with selected area electron diffraction (SAD). Figure 3 shows a bright field image and corresponding SAD pattern of a small representative  $\beta\text{W}_2\text{C}$  aggregate. Dominant feature of the pattern (Fig. 3b) is spots although diffuse ring pattern is barely seen. The square pattern of spots that belongs to the [100] zone axis shows that the {100} planes of  $\beta\text{W}_2\text{C}$  are predominantly oriented parallel to the flat aggregate as would be the case with a single crystal. Although a crystal of  $\text{WO}_3$  is broken into many 4 nm crystallites of  $\beta\text{W}_2\text{C}$  during the  $\text{WO}_3$ -to- $\beta\text{W}_2\text{C}$  transformation, these crystallites form an aggregate in which the position of a W atom in a crystallite relative to other W atoms, even in other crystallites, is not altered as far as the crystallites remained in the same aggregates. In other words, individual  $\beta\text{W}_2\text{C}$  crystallites comprising the aggregate maintain the same crystallographic relationship as in the starting  $\text{WO}_3$ , thus confirming the topotactic relationship to  $\text{WO}_3$ . The diffuse rings may arise from slight misorientation between the crystallites.

The image (Fig. 3a) shows a random mosaic of small domains along the edges of the aggregate. This type of image contrast is caused by density variation in the specimen and is commonly encountered in porous solids. Thus the material, originally non-porous, developed voids. Since large oxygen atoms are replaced by small carbon atoms maintaining relative positions of W atoms, a great reduction in specific volume per 1g of W must occur. This difference in specific volume must be balanced by developing pores. The sponge aggregate seen by TEM can be viewed as a

highly porous defect single crystal of  $\beta\text{W}_2\text{N}$ . All these TEM observations are very similar to those made previously for  $\text{MoO}_3$ -to- $\text{Mo}_2\text{N}$  transformation [4], and shows that the reactions involved in the preparation of  $\beta\text{W}_2\text{C}$  from  $\text{WO}_3$  belong to the class of topotactic solid transformation. Also as in the case of the  $\text{MoO}_3$ -to- $\alpha\text{MoC}_{1-x}$  transformation, the reason for the topotaxy in  $\text{WO}_3$ -to- $\beta\text{W}_2\text{C}$  transformation is believed to be the mild preparation conditions limiting the movement of W atoms during the transformation [5].

#### ACKNOWLEDGEMENT

Transmission Electron Microscopy in this study was performed at NASA Ames Research Center in Mountain View, California in collaboration with D.H. Su. This work has been supported by a KOSEF contract K82748.

#### REFERENCES

1. Levy, R. and Boudart, M.: *Science*, **181**, 547 (1973).
2. Boudart, M., Lee, J.S., Imura, K., and Yoshida, S.: *J. Catal.*, **103**, 30 (1987).
3. Lemaitre, J., Vidick, B., and Delmon, B.: *J. Catal.*, **99**, 415 (1986).
4. Volpe, L. and Boudart, M.: *J. Solid State Chem.*, **59**, 348 (1985).
5. Lee, J.S., Volpe, L., Ribeiro, F.H., and Boudart, M.: *J. Catal.*, **112**, 44 (1988).
6. Volpe, L. and Boudart, M.: *J. Solid State Chem.*, **59**, 332 (1985).
7. Lee, J.S., Ribeiro, F.H., and Boudart, M.: Submitted to *Catal. Lett.*
8. Kojima, I., Miyazaki, E., Inoue, Y., and Yasumori, I.: *J. Catal.*, **59**, 472 (1979).
9. Benziger, J.B., Ko, E.I., and Madix, R.J.: *J. Catal.*, **54**, 414 (1978).
10. Toth, L.E.: "Transition Metal Carbides and Nitrides", Academic Press, New York, 1971.
11. Sara, R.V.: *J. Am. Ceram. Soc.*, **48**, 251 (1965).
12. Oswald, H.R.; Gunter, J.R., "1976 Crystal Growth and Materials", E. Ka; dis, and H.J. Scheel, Eds., North Holland, Amsterdam, 1977, p.415.
13. Volpe, L. and Boudart, M.: *Catal. Rev.-Sci. Eng.*, **27**, 515 (1985).